Cancer Cell, Volume *16*

Supplemental Data

$CD4^+$ T Cells Regulate Pulmonary Metastasis of Mammary Carcinomas by Enhancing Protumor Properties of Macrophages

David G. DeNardo, Jairo B. Baretto, Pauline Andreu, Lesley Vasquez, David Tawfik, Nakita Kolhatkar, and Lisa M. Coussens

SUPPLEMENTAL DATA

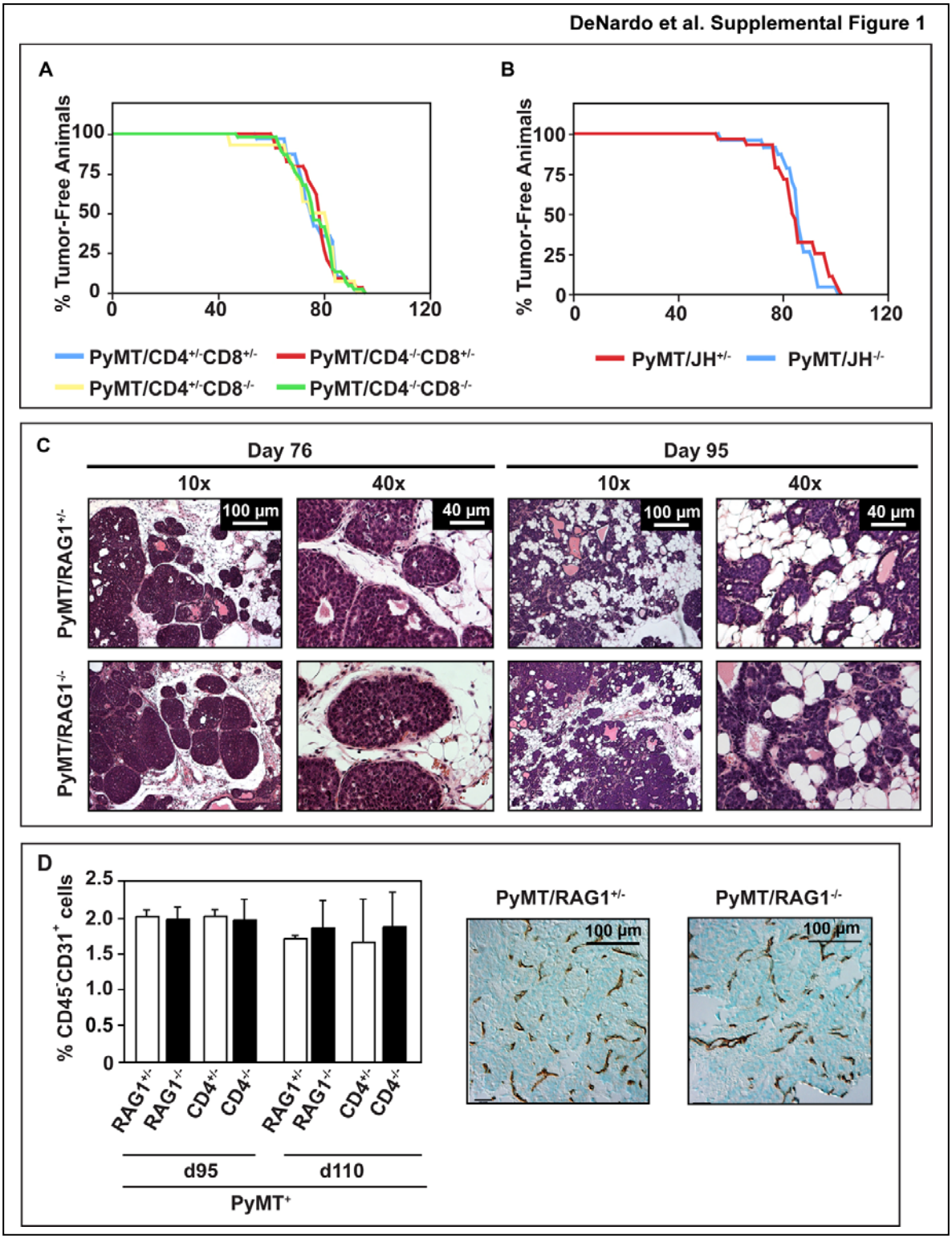

Figure S1: The impact of $CD4^+$ T cells on primary mammary tumor development

A-B) Kaplan Meyer analysis of tumor incidence in CD4, CD8 and B cell-deficient/*PyMT* mice. The percent of tumor free animals is depicted for *PyMT/CD4*$^{+/-}$*CD8*$^{+/-}$ (n=10), *PyMT/CD4*$^{-/-}$*CD8*$^{-/-}$ (n=46), *PyMT/CD4*$^{-/-}$*CD8*$^{+/-}$ (n=34), *PyMT/CD4*$^{+/-}$*CD8*$^{-/-}$ (n=31) as well as *PyMT/JH*$^{+/-}$ (n=23) and *PyMT/JH*$^{-/-}$ (n=28) mice. Animals were considered to be tumor free until a palpable mass (>4.0 mm) persisted for longer then 4 days. There were no statistical differences between tumor incidence curves by generalized Wilcoxon test.

C) Representative images of H&E stained mammary tumor tissue from 76 and 95-day old *PyMT/RAG1*$^{+/-}$ and *PyMT/RAG1*$^{-/-}$ mice. Magnification and scale are shown.

D) Flow cytometric analysis of $CD31^+$ endothelial cells in mammary tumors from 95 and 110 day-old *PyMT/RAG1*$^{+/-}$, *PyMT/RAG1*$^{-/-}$, *PyMT/CD4*$^{+/-}$*CD8*$^{+/-}$, *PyMT/CD4*$^{-/-}$*CD8*$^{-/-}$ mice (n=4). Data is depicted as the mean % $CD31^+$ cells of the total live cells/tumor ±SEM. No statistical differences were found between groups by Mann-Whitney test. Representative 20x images of paraffin embedded tumor sections from *PyMT/CD4*$^{+/-}$, *PyMT/CD4*$^{-/-}$ sections stained for $CD31^+$ and vasculature revealed as brown staining. Bar in both = 100 μm.

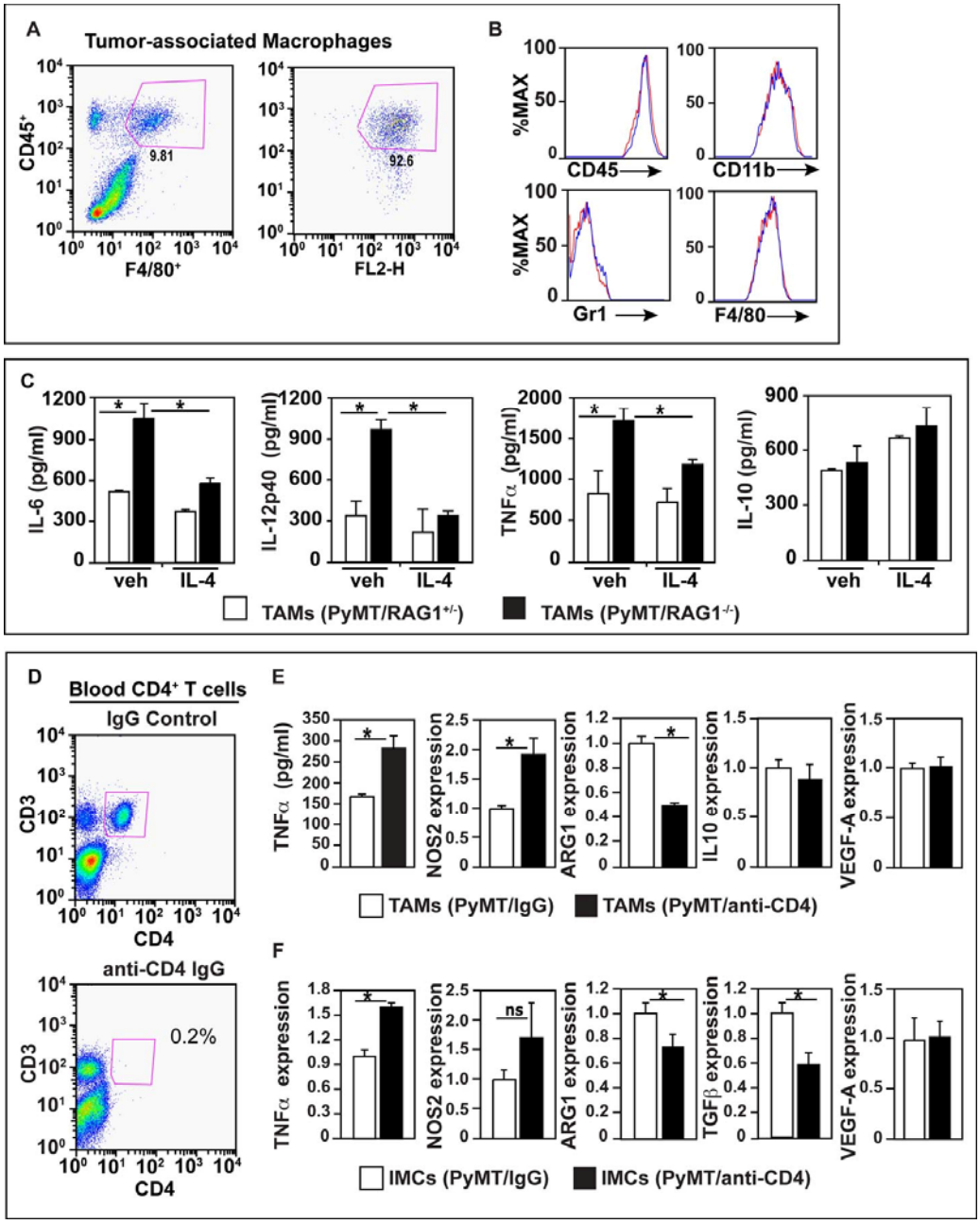

Figure S2: CD4$^+$ T lymphocytes regulate bioeffector function of myeloid cell subsets

A-B) Isolation of TAMs from the mammary tumors of *PyMT/CD4*$^{+/-}$ and *PyMT/CD4*$^{-/-}$ mice. The purity of isolated CD45$^+$F4/80$^+$Gr1$^-$ macrophages was assessed by flow cytometric analysis of the cell suspension before and after selection. Representative analyses are shown from *PyMT/CD4*$^{+/-}$(red) and *PyMT/*CD4$^{-/-}$ (blue) tumors and relative CD45, CD11b, Gr1 and F4/80 expression depicted.

C) Cytokine expression analysis from TAM-conditioned medium. Tumor-associated CD45$^+$F4/80$^+$Gr1$^-$ macrophages were isolated by dual magnetic and flow sorting of mammary tumors from 95 day-old

PyMT/RAG1$^{+/-}$ and *PyMT/RAG1*$^{-/-}$ mice (n=3/cohort). Cytokine expression was assessed by ELISA of conditioned medium from TAMs (25,000) following 18 hours of culture, with or without recombinant IL-4 (10 ng/ml). Representative assays from 2 independent cohorts each performed at least in triplicate are depicted as means ± SEM and * denotes $p<0.05$ by student t test.

D) Lymphocyte depletion by anti-CD4 IgG (GK1.1) was assessed by flow cytometric analysis 4 days after of IgG injection. Representative analyses from anti-CD4 IgG and control IgG treated mice are shown from blood isolated by left ventricle heart puncture. % $CD4^+$ of total cells is depicted.

E) Analysis of TAM polarization following $CD4^+$ T cells depletion. Tumor-associated $CD45^+F4/80^+Gr1^-$ macrophages were isolated by flow sorting mammary tumors from *PyMT* mice treated with either anti-CD4 IgG (GK1.1) or control IgG. Tumor bearing 85 day-old mice were treated twice over 10 days with Igs and TAMs were isolated from tumors when mice were 95 day-old. Cytokine expression was assessed by ELISA analysis of conditioned medium from TAMs following 18 hours of culture. Gene expression analysis used the comparative threshold cycle method to calculate fold change in gene expression normalized to *GAPDH* as reference gene. Representative assays from 2 independent cohorts each run at least in triplicate are depicted as mean values ± SEM. * denotes n $p<0.05$ by Mann-Whitney.

F) Analysis of IMC polarization following $CD4^+$ T cells depletion. Tumor-associated $CD45^+CD11b^+Gr1^{Hi}$ IMCs were isolated by flow sorting mammary tumors from *PyMT* mice treated with either anti-CD4 IgG (GK1.1) or control IgG. Tumor bearing 85 day-old mice were treated twice over 10 days with Igs and TAMs were isolated from tumors when mice were 95 day-old. Cytokine expression was assessed by ELISA and quantitative real-time PCR as described above. Representative assays from 2 independent cohorts each run at least in triplicate are represented as mean values ± SEM. * denotes $p<0.05$ by Mann-Whitney.

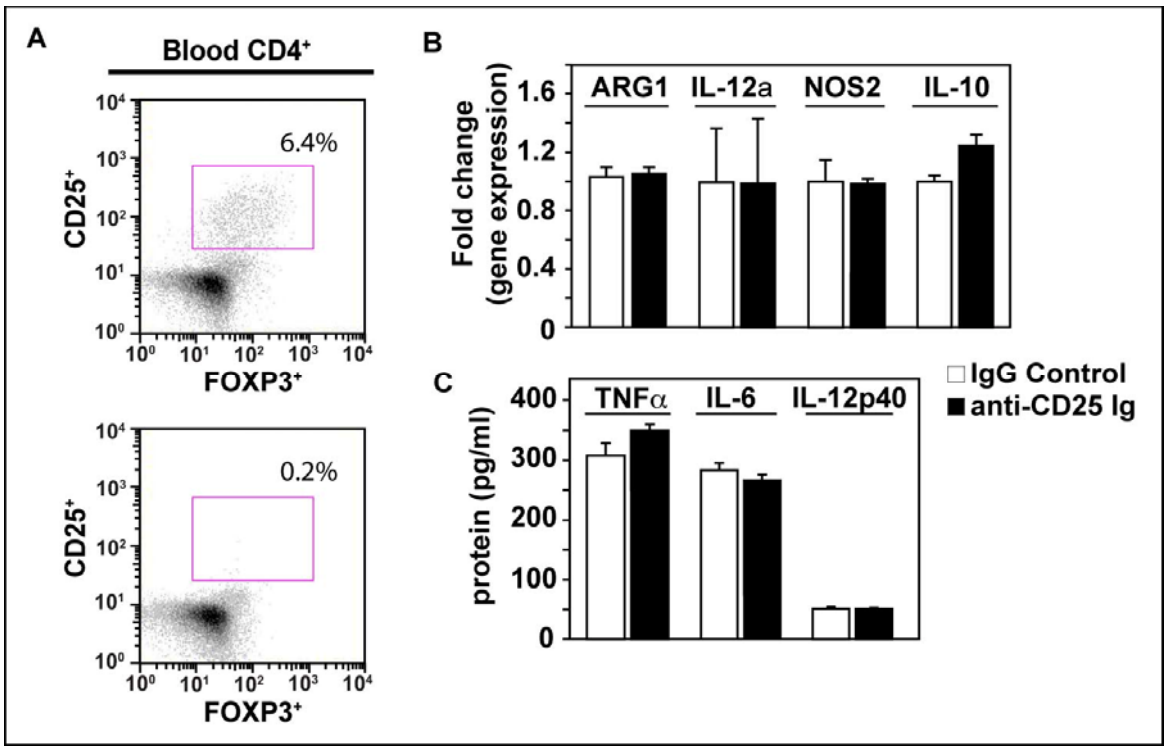

Figure S3: Cytokine profiles of TAMs from CD25 T_{reg}-depleted mice.

A) Analysis of $CD25^+$ T cell depletion. Tumor bearing 85 day-old *PyMT* mice (5 mice/cohort) were treated with either anti-CD25 IgG (PC61) or control IgG three times over 15 days. Peripheral blood was analyzed for expression of FOXP3 and CD25 expression on $CD4^+$ T lymphocytes every 5 days by flow cytometry to affirm depletion. Representative analysis for depleted versus control 100 day-old *PyMT* mice is depicted as FACS plots gated on $CD4^+$ lymphocytes.

B) Quantitative real-time PCR analysis of *Nos2, Arg1, Tgfβ, IL-12a* and *IL-10* mRNAs expression in tumor-associated $CD45^+F4/80^+Gr1^-$ macrophages isolated by flow sorting from mammary tumors of 100 day-old *PyMT* mice treated with either anti-CD25 Ig (PC61) or isotype control IgG. The comparative threshold cycle method was used to calculate fold change in gene expression normalized to *GAPDH* as reference gene. Cell isolation and gene expression analysis was performed on 2 separate cohorts of animals (3 mice/group) with similar results. Representative data are depicted as means ± SEM. No statistical differences were found between treated and untreated groups by Mann-Whitney.

C) Cytokine expression analysis from TAM conditioned medium. Tumor-associated $CD45^+F4/80^+Gr1^-$ macrophages were isolated by flow sorting from mammary tumors from 100 day-old *PyMT* mice treated with either anti-CD25 Ig (PC61) or isotype control IgG for 15 days. Cytokine

expression was assessed by ELISA analysis of conditioned medium from TAMs following 18 hours of culture. Cell isolation and cytokine analysis was performed on 3 separate cohorts of animals (2 mice/group) with similar results. Representative data are depicted as mean ± SEM. No statistical differences were found between treated and untreated groups by Mann-Whitney.

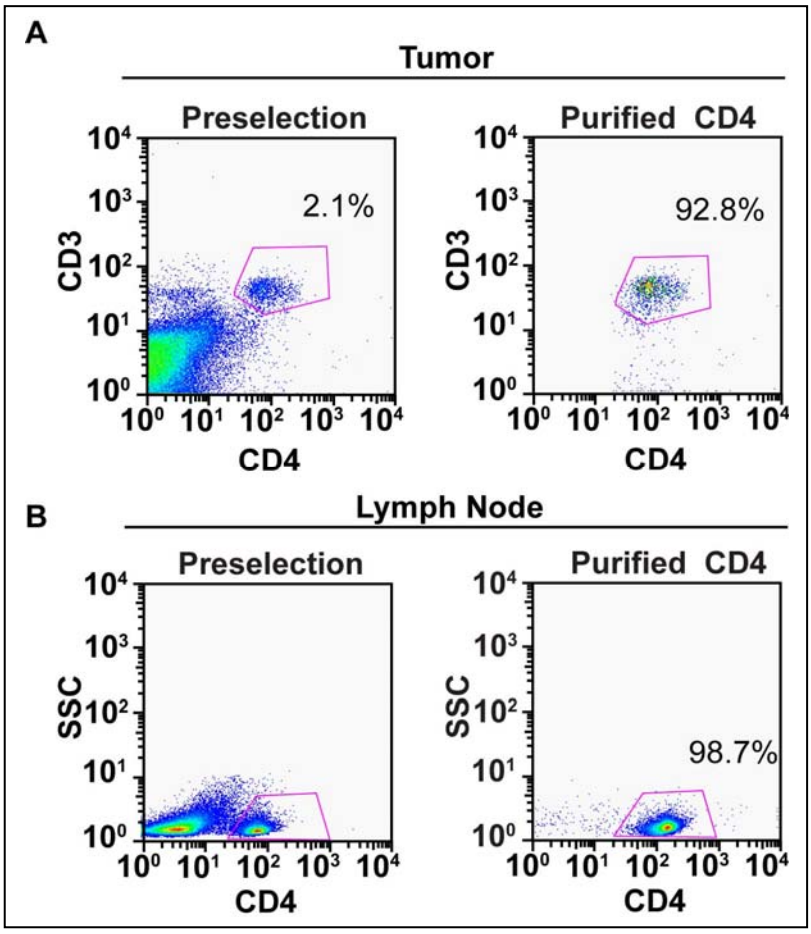

Figure S4. CD4 T lymphocyte purification and depletion.

A-B) Isolation of $CD4^+$ T lymphocytes from tumors and lymph nodes. Selection was done by magnetic selection for CD4 followed by FACS sorting for CD3 and CD4 positive cells. The purity of isolated cells was assessed by flow cytometric analysis of pre-selection and purified cells. Representative analyses are shown from tumor and LN isolations. % $CD4^+$ of total cells is shown.

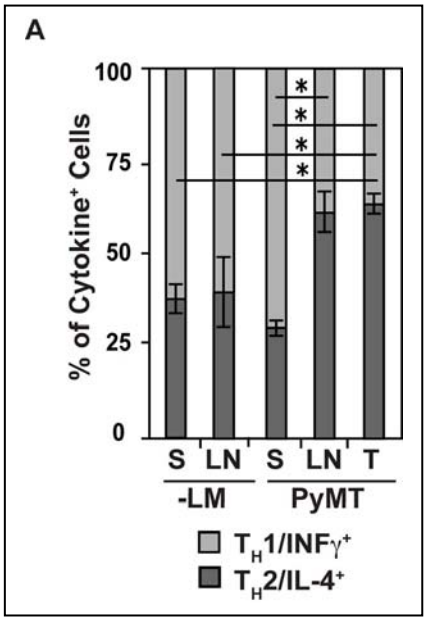

Figure S5. CD4$^+$ T lymphocytes are T_H2 polarized in primary mammary tumors

A) Analysis of intracellular cytokine expression by CD4$^+$ T cells. CD4$^+$ T cells were isolated by flow sorting from spleen (S), lymph nodes (LN) or tumors (T) from 95 day-old (-)LN or *PyMT* mice (n=3/cohort). Isolated CD4$^+$ T cells were activated *ex vivo* by treatment with anti-mouse CD3 and CD28 IgGs in the presence of Brefeldin A. Cells were fixed and intracellular IL-4 and IFNγ was calculated after 6 hours of activation. The Ratio of IL-4$^+$ to IFNγ$^+$ CD4$^+$ T cells is depicted as mean % of cytokine positive cells from 3 independent isolation experiments and * denotes $p<0.05$ by Mann-Whitney.

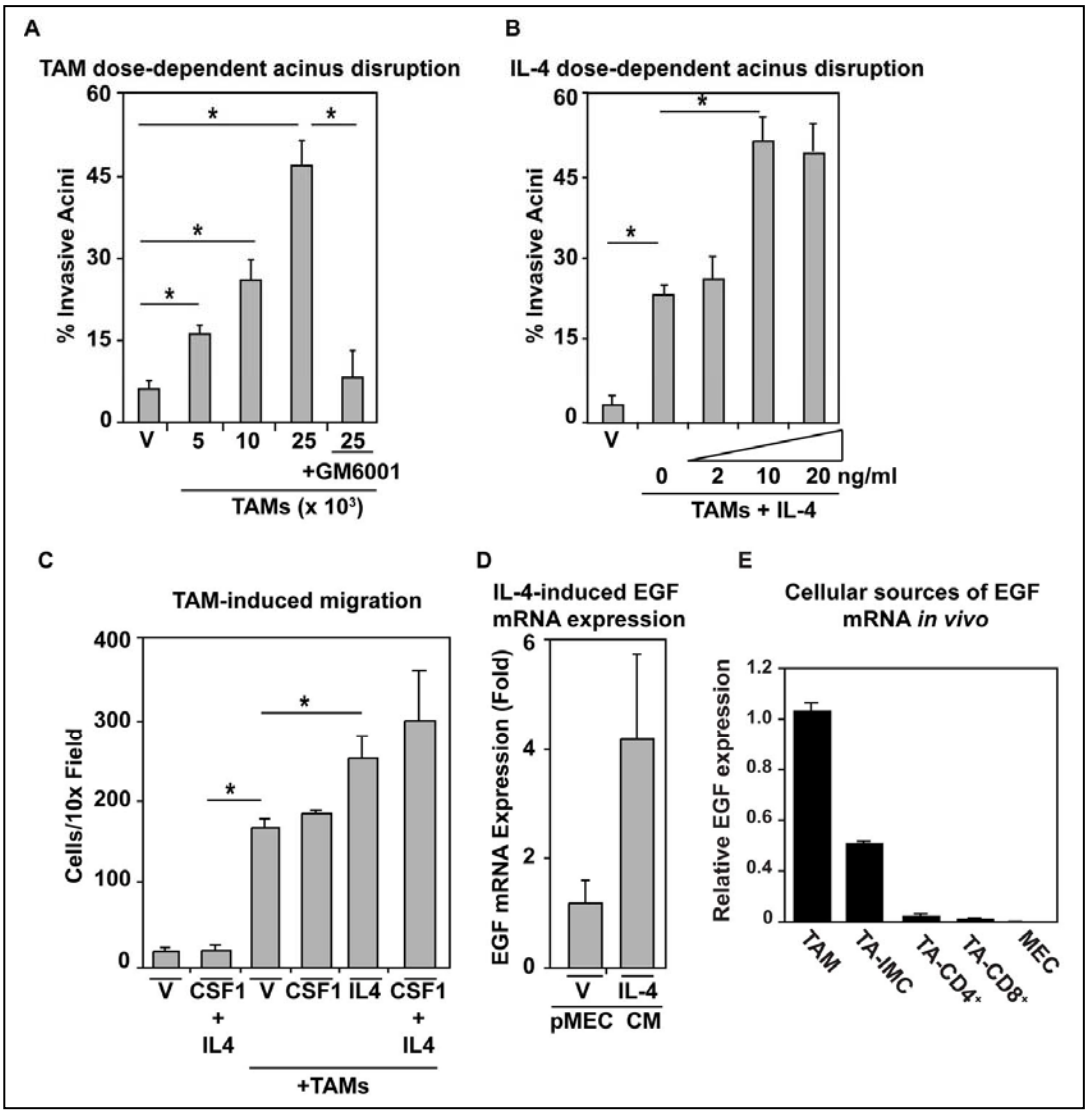

Figure S6: Alternatively activated TAMs induce malignant behavior.

A) Quantification of pMEC organoid disruption following co-culture with TAMs (isolated from mammary tumors of 95 day-old *PyMT* mice). Metalloprotease activity was inhibited by treatment with a broad-spectrum MMP inhibitor GM6001 (10 μM). Disrupted organoids were quantified and data represented as a percentage of total organoids (>100 replicate/4 replicates). Data depicted as mean ± SEM and * denotes $p<0.05$ by Mann-Whitney.

B) Quantification of organoid disruption following co-culture of TAM (48 hours) with pMEC, in the presence of either vehicle (V) or increasing concentrations of IL-4 (2-20 ng/ml). Disrupted organoids were counted and then expressed as a percentage of the total organoids present. Disrupted organoids

were counted and data represented as a percentage of the total organoids (>100 replicate/4 replicates). Data depicted as mean ± SEM and * denotes $p<0.05$ by Mann-Whitney.

C) Quantification of pMEC migration/chemotaxis in response to TAMs treated with IL-4 (10 ng/ml) and/or CSF-1 (10ng/ml) assessed using a Boyden chamber assay. The number of pMECs that migrated to the opposite side of the membrane was assessed by H&E staining, four 10x fields were quantified per membrane (using Image J) and 4 inserts were used for each condition. Data are represented as mean ± SEM and * denotes $p<0.05$ by Mann-Whitney.

D) Quantitative real-time PCR analysis for *EGF* mRNA expression from $CD45^{+}F4/80^{+}Gr1^{-}$ macrophages isolated by flow sorting from mammary tumors from 95 day-old *PyMT/CD4*$^{+/-}$ mice. TAMs were with treated pMEC conditioned medium (24 hours conditioning) with or without IL-4 (20 ng/ml). The comparative threshold cycle method was used to calculate fold change in gene expression normalized to *β-actin* as a gene reference. Representative data from 2 independent experiments is depicted as the mean fold change from the standardized sample ± SEM. In all panels, * denotes $p<0.05$ by Mann-Whitney.

E) Macrophages as a source of EGF in mammary carcinomas. Quantitative real-time PCR analysis of *EGF* mRNA expression in tumor-associated $CD45^{+}F4/80^{+}Gr1^{-}$ macrophages (TAMs), $CD45^{+}CD11b^{+}Gr1^{HI}$ IMCs, $CD4^{+}$ and $CD8^{+}$ T cells as well as MECs from mammary carcinomas of 100 day-old *PyMT* mice isolated by flow sorting. The comparative threshold cycle method was used to calculate fold change in gene expression normalized to *GAPDH* as reference gene. Cell isolation and gene expression analysis was performed on 4 separate cohorts of animals (1-2 mice/cohort). Representative data are depicted as mean ± SEM.

SUPPLEMENTAL EXPERIMENTAL PROCEDURES:

ELISA

TNFα, IL-6, IL-1b, IL-12, IL-4, IL-17 and IFNγ concentrations of conditioned medium were assayed using Ready-Set-Go ELISA kits (eBioscience) and IL-10 assessed using a quantikine immunoassay (BD Bioscience) as described by the manufacturer. Optical density was measured at 450 nm with wavelength correction set to 540 nm on a SpectraMax 340 spectrophotomoter (Molecular Devices).

Quantitative RT-PCR

Total RNA was extracted from 200-300,000 FACS sorted $CD45^{+}F4/80^{+}Gr1^{-}$ cells using an RNeasy Mini Kit (QIAGEN). cDNAs were synthesized using Superscript III^{tm} First-strand synthesis (Invitrogen). Primers specific for *β-actin, GAPDH EGF, Vegf-a, MMP-9, Tgfβ, Arignase-1, and Nos2* (Superarray) were used and relative gene expression was determined using RT^2 Real-Time^{tm} SYBR Green/ROX PCR master mix (Superarray) on an ABI 7900HT quantitative PCR machine (ABI biosystems). The comparative threshold cycle method was used to calculate fold change in gene expression, which was normalized to both *β-actin* and *Gapdh* as reference genes. Samples were assayed from at least three independent experiments per category.

Flow cytometric analysis

Single-cell suspensions were prepared from mammary gland dissection by manual mincing using scalpel followed by enzymatic digestion for 40 min at 37°C by Collagenase A 3.0 mg/ml (Roche) and DNase I (Roche) dissolved in DMEM (Invitrogen), under stirring conditions. Digestion mixtures were quenched by adding DMEM containing 10% FBS and then filtered through 0.7 μm nylon strainers (Falcon). Cells were then incubated for 10 min at 4°C with rat anti-mouse CD16/CD32 mAb (BD Biosciences) at a 1:100 dilution in PBS containing 1% of BSA (Sigma) to prevent nonspecific antibody binding. Subsequently, cells were washed twice in PBS/BSA and incubated for 20 min with primary antibody (1:100) followed by two washes with PBS/BSA. 7-AAD (BD Biosciences) was added (1:10) to discriminate between viable and dead cells. Data acquisition and analysis were performed on a FACSCalibur using CellQuestPro software (BD Biosciences).

Tumor and metastatic burden

Tumor burden was determined by caliper measurements on live sedated mice at day 95 and day 110.

Metastatic disease was assessed by serial sectioning of formalin-fixed paraffin-embedded lungs. Entire lungs were sectioned and number of metastatic foci (>5 cells) counted on 6 sections taken every 100 μm following staining with hematoxylin and eosin (H&E). 15 to 30 lungs were analyzed for each cohort indicated.

Immunohistochemistry

Paraffin-embedded tissue sections were fixed in 10 % formalin and incubated with detection antibodies as previously described (Junankar et al., 2006). A biotinylated secondary antibody was applied, followed by incubation with streptavidin-conjugated HRP. Peroxidase activity was localized with diaminobenzidine (Vectastain ABC kit, Vector Laboratories). For immunofluorescent staining Alexa fluor 594 conjugated goat anti-rat (Molecular Probes, 10 mg/ml) was used. All immuno-localization experiments were repeated on multiple tissue sections and included negative controls for determination of background staining, which was negligible. Quantitative analysis of $CD4^+$ and $F480^+$ cells was performed by counting cells in ten high-power fields (20×) per age-matched tissue section from five mice per group. IHC analysis of human breast tissue was accomplished using commercially available tissue microarrays (Pantomics BRC150101, 2, 3). Citrate antigen retrieval (BioGenex) was used for CD4 and CD8 staining and Proteinase XXV (Lab Vision) for CD68. Following blocking in Goat serum, Ab dilutions of 1:25 CD4 (4B12, Novocastra), 1:100 CD68 (KP1, Neomarkers) and CD8 (C8/144B, Neomarkers) were then applied. Appropriate biotinylated secondary antibody was applied, followed by incubation with streptavidin-conjugated HRP. Peroxidase activity was localized with diaminobenzidine (Vectastain ABC kit, Vector Laboratories). The mean number of positive cells in tissue section was evaluated by counting all high power fields (20x) per tissue section (1.1 mm)/ 2 sections/patient using Image J (NIH).

Immune cell isolation

Immune cells were isolated from tumors using a dual purification strategy including magnetic purification followed by flow sorting. Single cell suspensions from tumors were created as described above. Alternatively, single cell suspensions generated from lymph nodes or spleens were passed through 0.7 μm nylon strainers (Falcon). Cells were then incubated for 10 min at 4°C with rat anti-mouse CD16/CD32 mAb (BD Biosciences) at a 1:100 dilution in PBS/BSA then washed twice in PBS/BSA and incubated for 20 min with appropriate fluorescent primary antibodies which included

anti-CD45-APC (30-F11), in addition to anti-CD4 (GK1.1), -CD3 (145-2C11), -Gr-1 (RB6-8G5), -CD11b (93) and/or F4/80 (BM8) (all from eBiosciences) at 1:100 dilution depending on the population to be isolated. Total leukocytes were isolated using magnetic bead selection for APC^+ according to manufactures specifications (Miltenyi Biotec). Magnetically selected cells were then flow sorted on a FACSAria using CellQuestPro software (BD Biosciences).

T cell activation

Dual magnetic and flow-sorted $CD45^+CD3^+CD4^+$ T lymphocytes were added to CD3/CD28 coated plates (5.0 μg/ml, eBioscience). Golgistop (BD Bioscience) was added to the medium and 8 hours later, conditioned medium was isolated and cells stained for CD4 using APC-conjugated anti-mouse CD4 (eBioscience) and then intracellularly with PE-conjugated anti-mouse IFNγ or FITC-conjugated anti-mouse IL-4 using the Cytofix/Cytoperm kit (BD Biosciences).

Supplemental References:

Junankar, S., Eichten, A., Kramer, A., de Visser, K. E., and Coussens, L. M. (2006). Analysis of immune cell infiltrates during squamous carcinoma development. J Invest Dermatology *126 Suppl*, 36-43.